New Phytologist

***New Phytologist* Supporting Information**

Article title: A homologue of the mammalian tumour suppressor protein PTEN is a functional lipid phosphatase and required for chemotaxis in filamentous fungi

Authors: Berit Hassing, Aleysha Candy, Carla J. Eaton, Tania R. Fernandes, Carl H. Mesarich, Antonio Di Pietro, Barry Scott

Article acceptance date: Click here to enter a date.

The following Supporting Information is available for this article:

New Phytologist

Table S2: Primers used in this study.

Methods S1: Construct design.

a

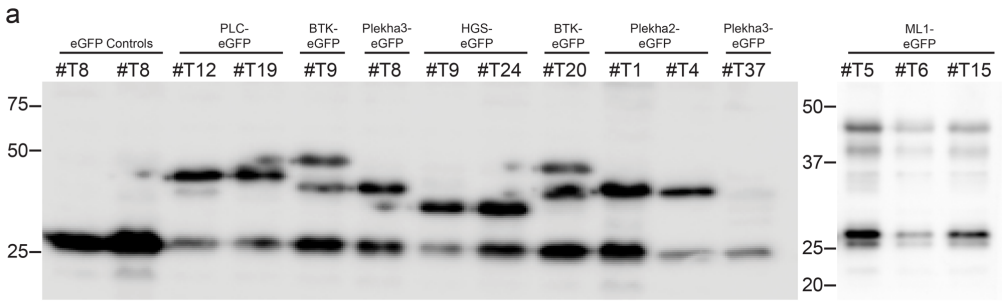

b

Construct	Domain Type	Phospholipid	Strain	Predicted MW (KDa)
eGFP	Control		8	29.95
PLC-eGFP	PH	$PI[4,5]P_2$	12	42.34
			19	
BTK-eGFP	PH	$PI[3,4,5]P_3$	9	47.13
Plekha3-eGFP	PH	PI[4]P	8	38.19
HGS-eGFP	FYVE	PI[3]P	9	32.26
			24	
BTK-eGFP	PH	$PI[3,4,5]P_3$	20	47.13
Plekha2-eGFP	PH	$PI[3,4]P_2$	1	40.01
			4	
Plekha3-eGFP	PH	PI[4]P	37	38.19
ML1-eGFP	N-terminal lipid binding domain	$PI[3,5]P_2$	5	43
			6	
			12	

c

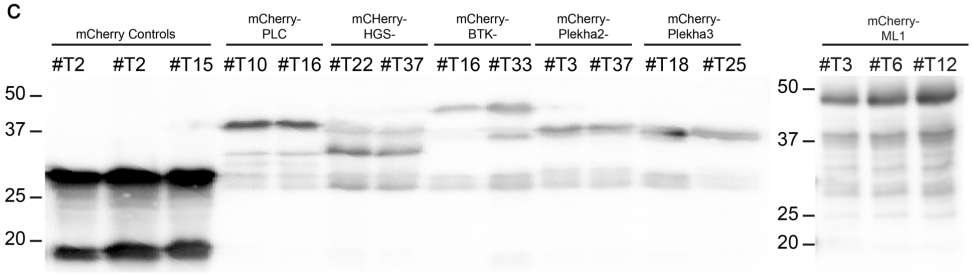

d

Construct	Domain Type	Phospholipid	Strain	Predicted MW (KDa)
mCherry	Control		2	26.73
			15	
mCherry-PLC	PH	$PI[4,5]P_2$	10	42.04
			16	
mCherry-HGS	FYVE	PI[3]P	22	34.97
			37	
mCherry-BTK	PH	$PI[3,4,5]P_3$	16	46.84
			33	
mCherry-Plekha2	PH	$PI[3,4]P_2$	3	39.72
			37	
mCherry-Plekha3	PH	PI[4]P	18	38.03
			25	
mCherry-ML1	N-terminal lipid binding domain	$PI[3,5]P_2$	4	42.78
			6	
			16	

Fig. S1: Verification of the expression of molecular probes in *Epichloë festucae* by western blot analysis.

(a) Western blot of total protein extract of lipid-binding molecular probe-expressing strains probed with the anti-GFP antibody (Abcam). Total protein extract of strain PN4175 expressing cytosolic eGFP (pCT74) was used as a control. For each strain, 50 µg of total protein was loaded and samples separated on a 10% SDS PAGE gel. (b) Table of molecular probe constructs and their expected molecular weight (kDa) as calculated using https://www.bioinformatics.org/sms/prot_mw.html. (c) Western blot of total protein extract of lipid-binding molecular probe-expressing strains probed with the anti-mCherry antibody (Abcam). For each strain, 50 µg of total protein was loaded and samples were separated on a 10% SDS PAGE gel. (d) Table of molecular probe constructs and their expected molecular weight (kDa) as calculated using https://www.bioinformatics.org/sms/prot_mw.html.

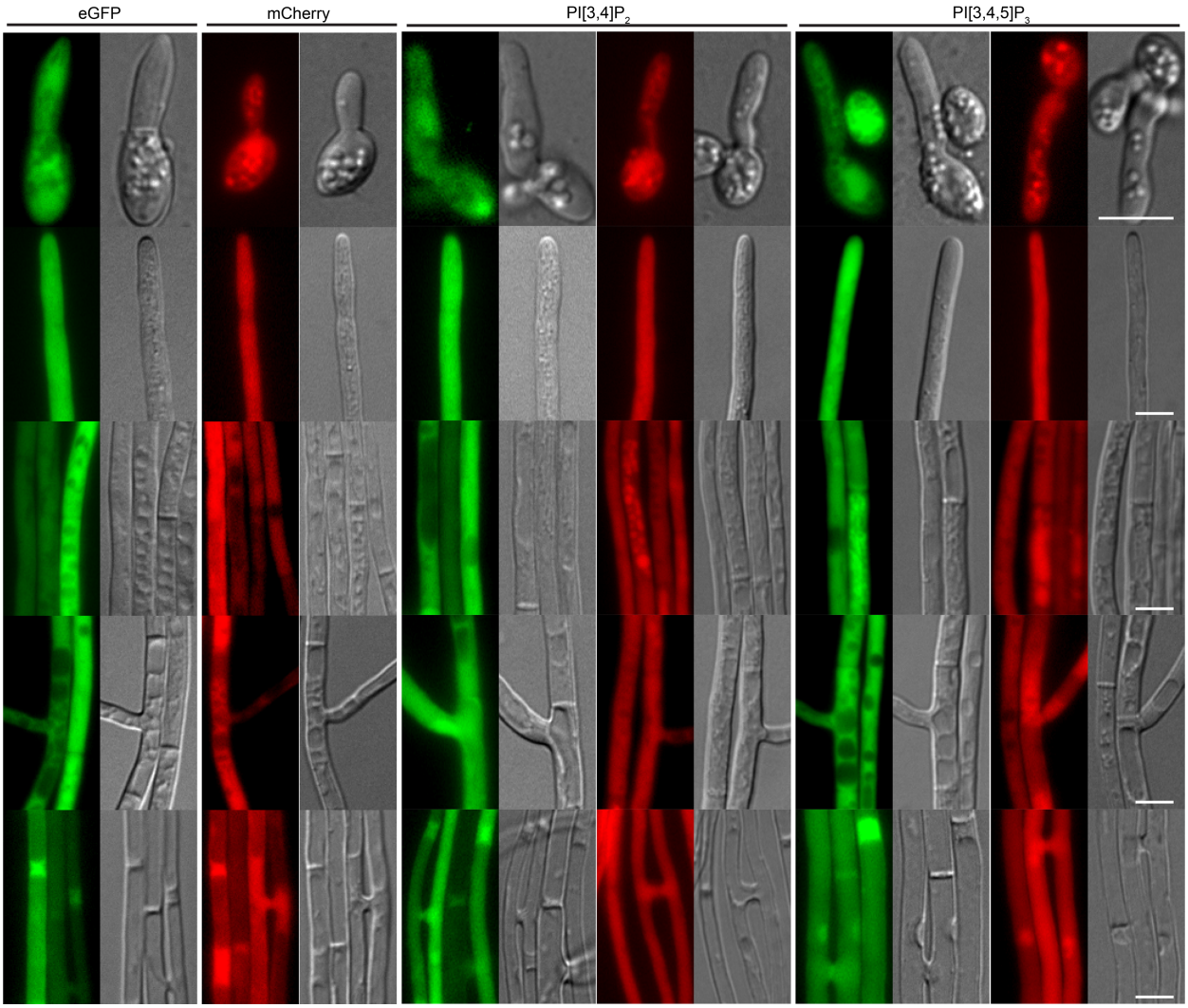

Fig. S2: Localisation of the PI[3,4]P_2 and PI[3,4,5]P_3 molecular probes in *Epichloë festucae* grown in axenic culture.

Strains were grown on 1.5% H_2O agar for 5 d before examination using a fluorescence microscope. Images shown are representative of all strains analysed and show localization of the molecular probes in hyphae of different ages. Images of spores were acquired from *E. festucae* E2368 transformants, whereas all others are from Fl1. Cytosolic eGFP (pCE25): #T5 (E2368), #T8 (Fl1); cytosolic mCherry (pCE126): #T7 (E2368), #T2 (Fl1); Plekha2-eGFP (PI[3,4]P_2 (pCE108): #T7 (E2368), #T1 (Fl1); mCherry-Plekha2 (PI[3,4]P_2, pCE113): #T6 (E2368), #T37 (Fl1); BTK-eGFP (PI[3,4,5]P_3, pCE107): #T14 (E2368), #T9 (Fl1); mCherry-BTK (PI[3,4,5]P_3, pCE112): #T1 (E2368), #T16 (Fl1); Bar = 5 µm.

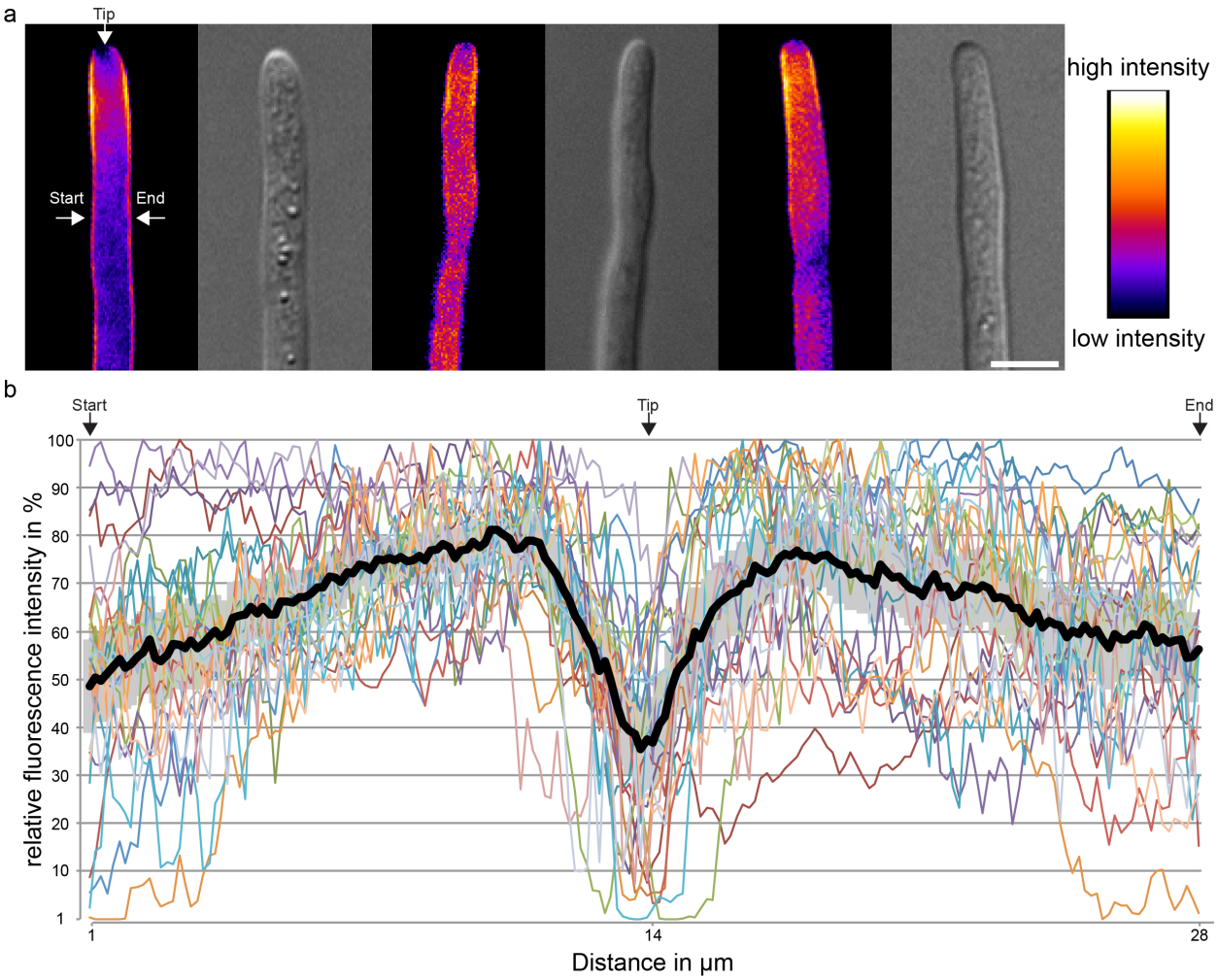

Fig. S3: Asymmetric distribution of the PI[4,5]P_2 molecular probe at the *Epichloë festucae* hyphal tip.

(a) Representative differential interference contrast and fluorescent microscopy images of the PI[4,5]P_2 biosensor at hyphal tips, pseudocoloured to indicate the saturation of each pixel from 0 to 255 (fully saturated). A three-pixel-wide line was drawn along the cell membrane from the start arrow around the tip to the end arrow. Graphs represent the concentration of biosensor along this line. Cultures were grown on 1.5% (w/v) water agar for 6-9 d. Bar = 5 µm. (b) Scatter graph summarising the concentration of the PI[4,5]P_2 biosensor along the cell membrane of 24 hyphal tips. Black line = trend line.

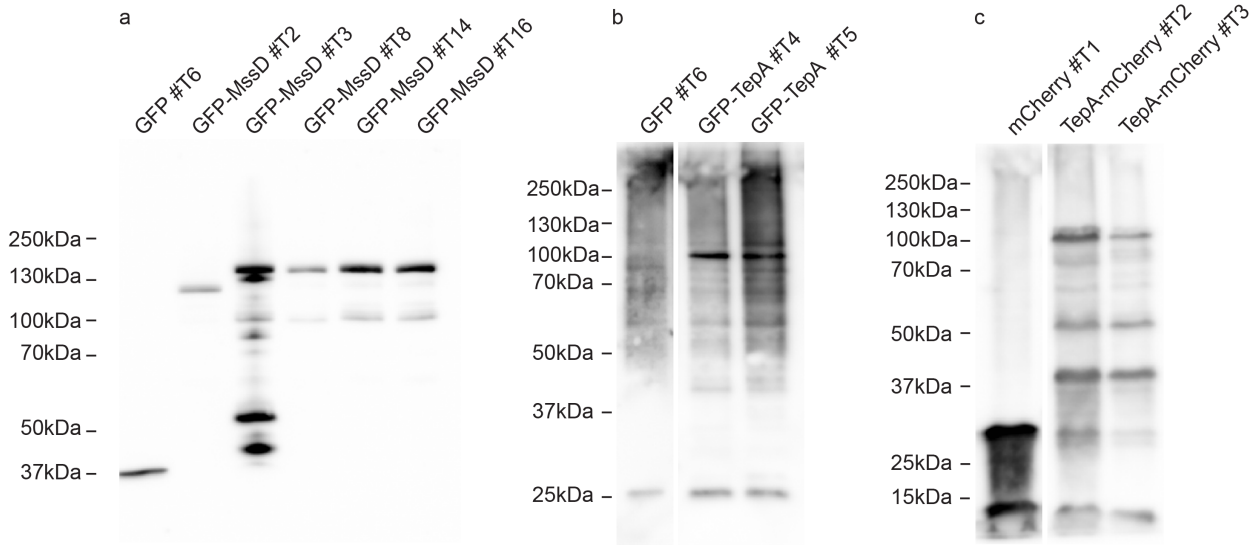

Fig. S4: Verification of the expression of eGFP-MssD, eGFP-TepA and TepA-mCherry fusion proteins in *Epichloë festucae* by western blot analysis.

Strains expressing the fusion proteins were incubated in liquid media for 3 d and total protein extracted. Approx. 15 µl of protein extract was loaded onto a 10% SDS acrylamide gel, separated and transferred onto PVDF membrane. Following transfer, membranes were probed with anti-GFP or anti-mCherry antibodies (Abcam), respectively. Following the incubation with a secondary anti-rabbit antibody (Abcam) conjugated to horseradish peroxidase (HRP), western blots were developed using a chemiluminescence reaction. All controls and fusion-protein constructs were expressed in the WT background, and the detection of eGFP (GFP#T6), eGFP-fusion proteins (eGFP-TepA#T4 and eGFP-TepA#T5), mCherry (mCherry#T1) and mCherry-fusion proteins (TepA-mCherry#T2 and #T3) is shown. The eGFP and mCherry expression controls are the same as previously described in Hassing *et al*. 2019 as they were run on the same gel. Expected protein sizes: GFP: 27 kDa; mCherry: 28.8 kDa; GFP-TepA: 86.18 kDa; TepA-mCherry: 87.98 kDa.

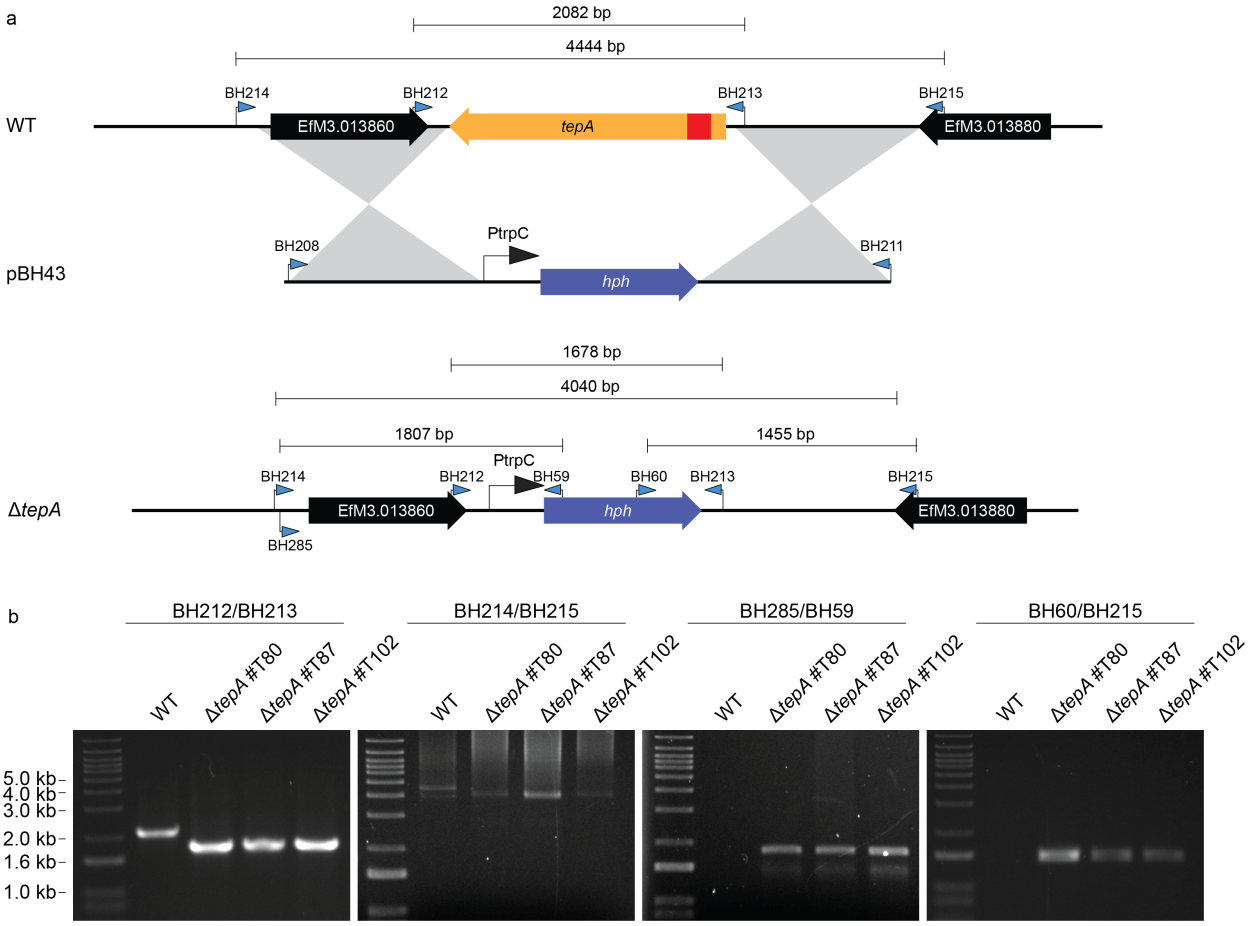

Fig. S5: Targeted replacement of the *Epichloë festucae tepA* gene.
(a) Physical map of the *tepA* wild-type (WT) genomic locus, linear insert of the *tepA* replacement construct, pBH43, and the mutant locus. Grey shading indicates regions of recombination. Numbers indicate the PCR primer pairs used for Gibson assembly (BH208/BH211) and deletion mutant screening (BH59/BH60/ BH212/BH213/BH214/BH215/BH285). (b) PCR screening of deletion candidates with the PCR primer pair BH212/BH213, generated expected bands of approx. 1.7 kb for the deletion mutants and approx. 2.1 kb for the WT strain. The primer pair BH214/BH215 generated expected bands of approx. 4.0 kb for the deletion mutants, and 4.4 kb for the WT strains. The primer pair BH60/BH215 generated a band of 1.5 kb and the primer pair BH285/BH59 a band of approx. 1.8 kb for the deletion mutants.

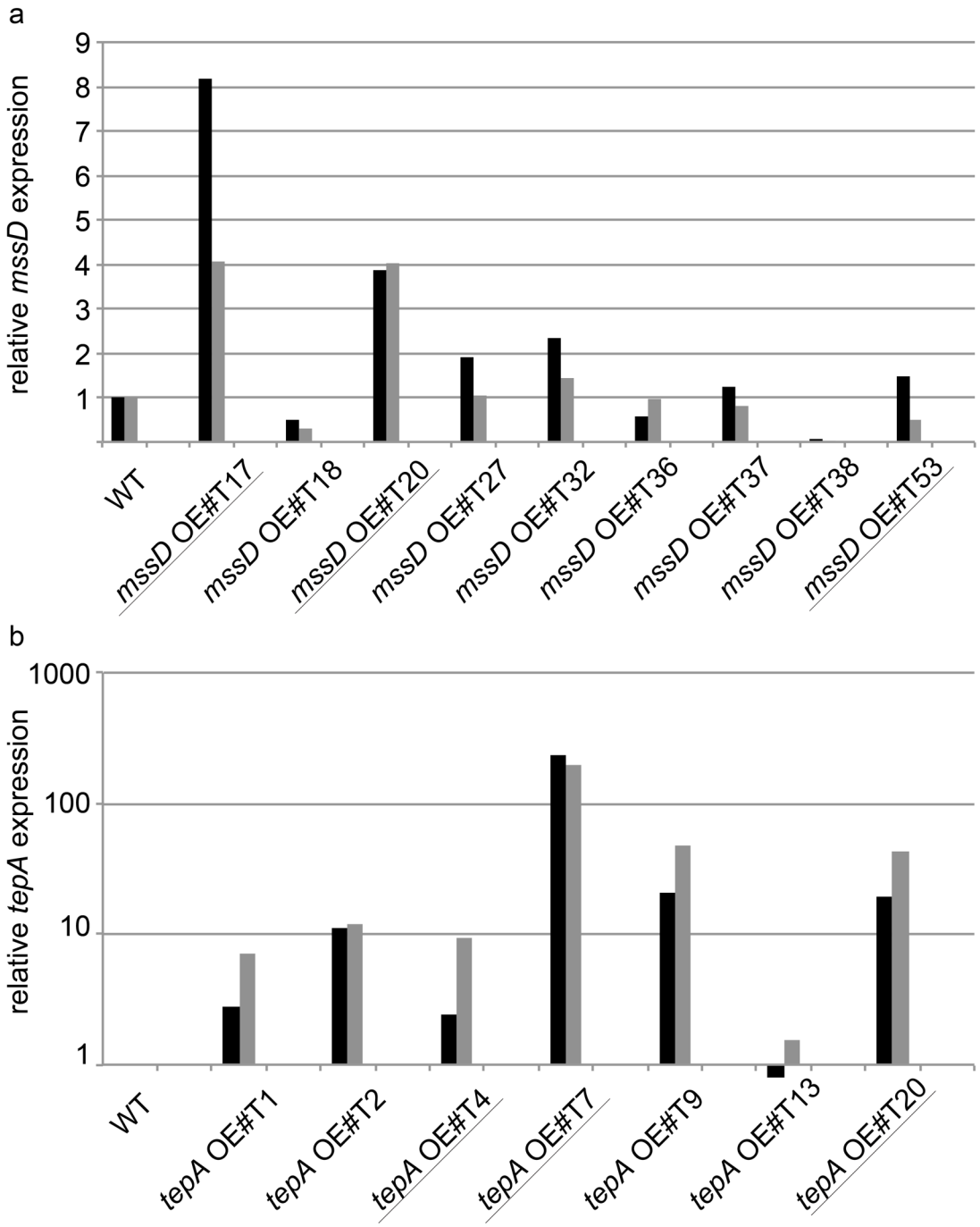

Fig. S6: Expression analysis of *Epichloë festucae mssD* and *tepA* overexpression strains by RT-qPCR.

Expression of *mssD* (a) and *tepA* (b) was determined relative to the wild-type (WT) expression using genes coding for elongation factor 2 (*EF-2*, black bar) and 40S ribosomal protein S22 (*S22*, grey bar) for normalisation with two technical replicates. For the amplification of *mssD*, the primer pair AC33/43, and for *tepA*, the primer pair BH189/199, was used. The relative expression was calculated as previously described (Lukito et al., 2015). Overexpression (OE) strains chosen for further analysis are underlined. Note the different scales on the y-axis.

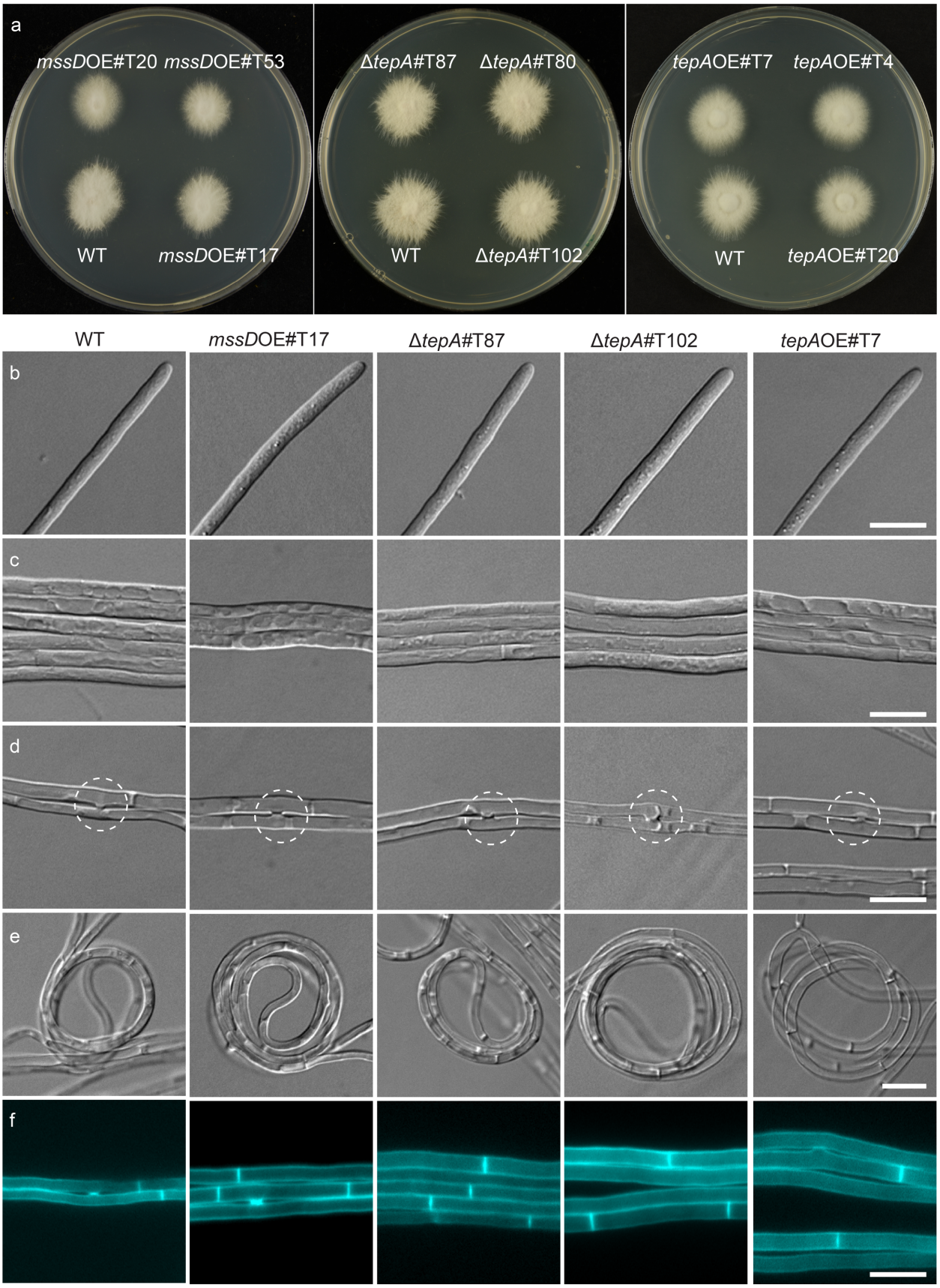
a
mssDOE#T20
mssDOE#T53
WT
mssDOE#T17
ΔtepA#T87
ΔtepA#T80
WT
ΔtepA#T102
tepAOE#T7
tepAOE#T4
WT
tepAOE#T20
WT
mssDOE#T17
ΔtepA#T87
ΔtepA#T102
tepAOE#T7
b
c
d
e
f

Fig. S7: Culture phenotype of *Epichloë festucae* wild-type, *mssD* overexpression and *tepA* deletion and overexpression mutants.
Wild-type (WT), *mssD* overexpression strains (#T17, #T20, #T53), *tepA* deletion strains (#T80, #T87, #T102) and *tepA* overexpression (OE) strains (#T4, #T7, #T20) were analysed multiple times. The images shown were captured of *mssD* OE #T17, Δ*tepA* #T87, Δ*tepA* #T102 and *tepA* OE #T7 and are representative of all strains analysed. (a) Whole colony morphology of WT and mutant strains grown on 2.4% PD agar for 7 d before examination; (b-f) strains were grown for 7 d on 1.5% H_2O agar before analysis; (b) Hyphal tip morphology in WT and mutant strains; (c) Formation of hyphal bundles in WT and mutant strains; (d) Hyphal fusion in WT and mutant strains; (e) Hyphal coil formation in WT and mutant strains; (f) Typical staining of hyphal bundle with Calcofluor white (CFW). White circle: hyphal fusion; Bar = 10 µm.

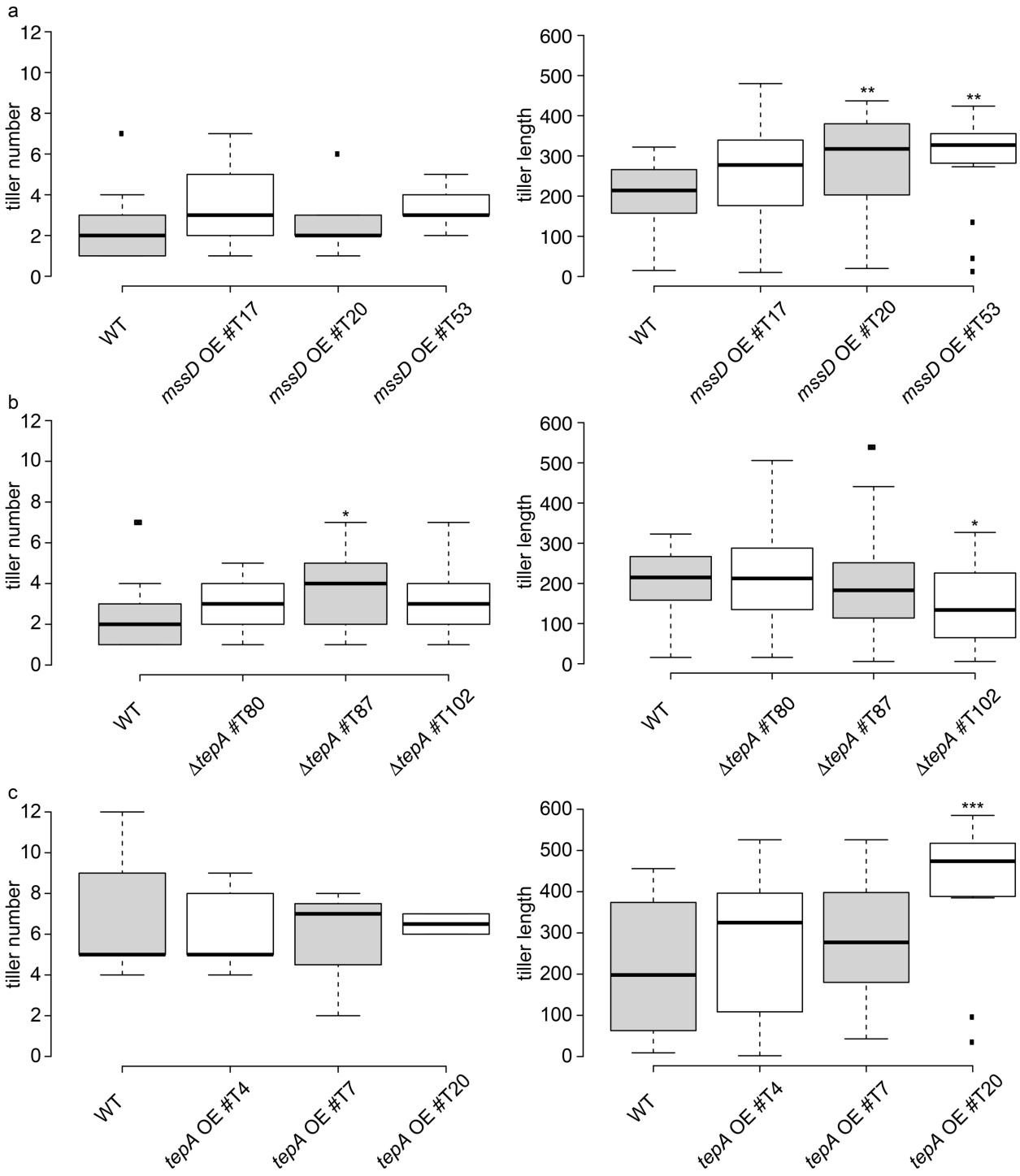

Fig. S8: Growth analysis of *Lolium perenne* plants infected with *Epichloë festucae* wild-type and *tepA* overexpression strains.

Tiller number of infected plants: wild-type (WT) (23), *mssD* overexpression strains #T17, #T20, #T53 (n=18/15/6), *tepA* deletion strains #T80, #T87, #T102 (n=31/32/18), WT (5), *tepA* overexpression strains #T4, #T7, #T20: (n=5/3/2). Box plots were generated using BoxPlotR (available on http://shiny.chemgrid.org/boxplotr/). One-way ANOVAs were used to test for differences in plant phenotypes between WT and mutant strains. In each case, the ANOVA was

fitted with R and a Bonferroni correction was applied to all *p*-values to account for multiple testing: *$p \leq 0.05$; **$p \leq 0.01$; ***$p \leq 0.001$. All other differences are not significant. The highly significant difference regarding the tiller length of the *tepA* OE strain #T20 has not been mentioned in the main text due to the low and therefore statistically insignificant number of biological replicates.

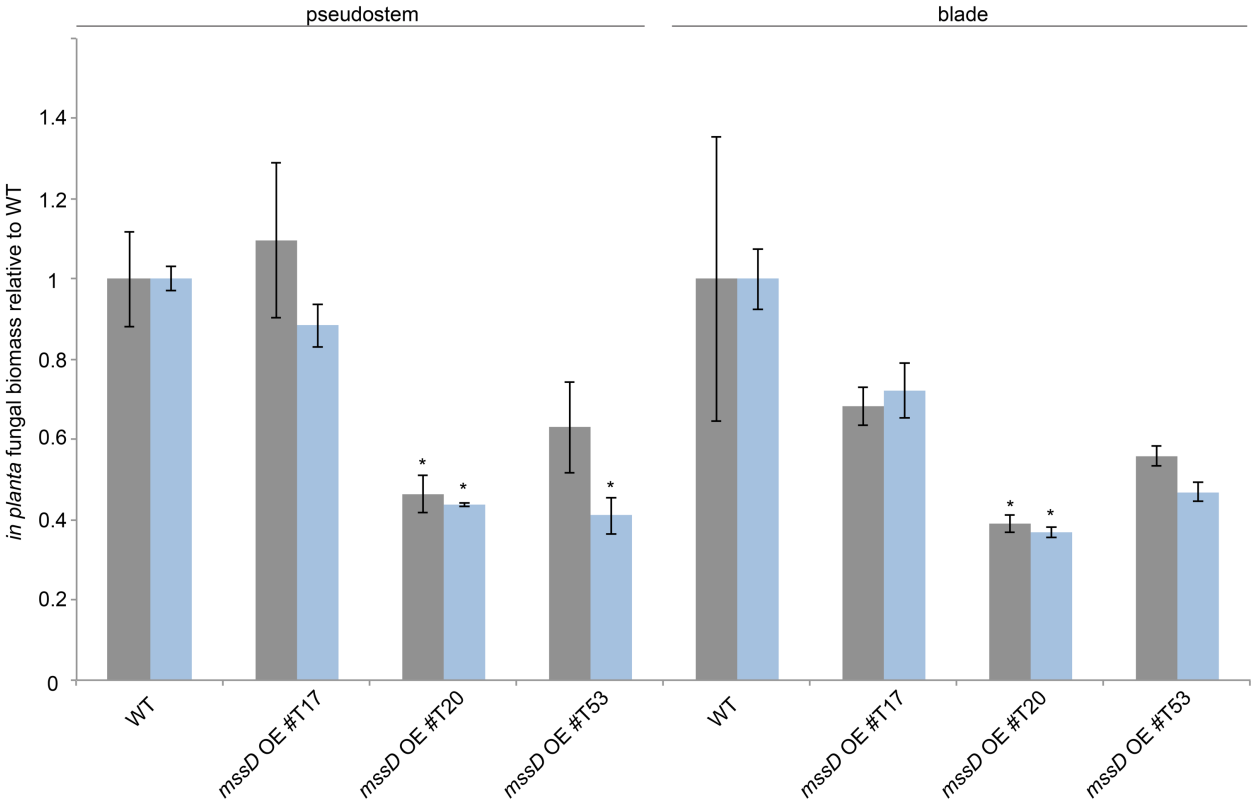

Fig. S9: Analysis of the *in planta* fungal biomass of *Epichloë festucae* wild-type and *mssD* overexpression strains.

The fungal biomass was analysed in three biological replicates of mature, infected *L. perenne* plants and is depicted relative to the WT biomass in the corresponding dataset. Grey bars show the relative biomass based on the presence of the fungal gene *hepA* (YL120F/YL120R) relative to the *L. perenne* gene *LpCCR1* (YL501F/YL501R) and blue bars the relative biomass based on the presence of the fungal gene *pacC* (YL113F/YL113R) relative to the *L. perenne* gene *LpCCR1* (YL502F/YL502R). Error bars represent the standard error. Asterisks represent statistically significant differences in the mutant-infected plants ($p \leq 0.05$) compared to the corresponding WT-infected plants calculated by a two-tailed Student *t*-Test. While the biomass was always significantly lower in *mssD* OE #T20-infected plants compared to WT-infected plants, the fungal biomass was only occasionally significantly reduced in *mssD* OE #T53-infected plants.

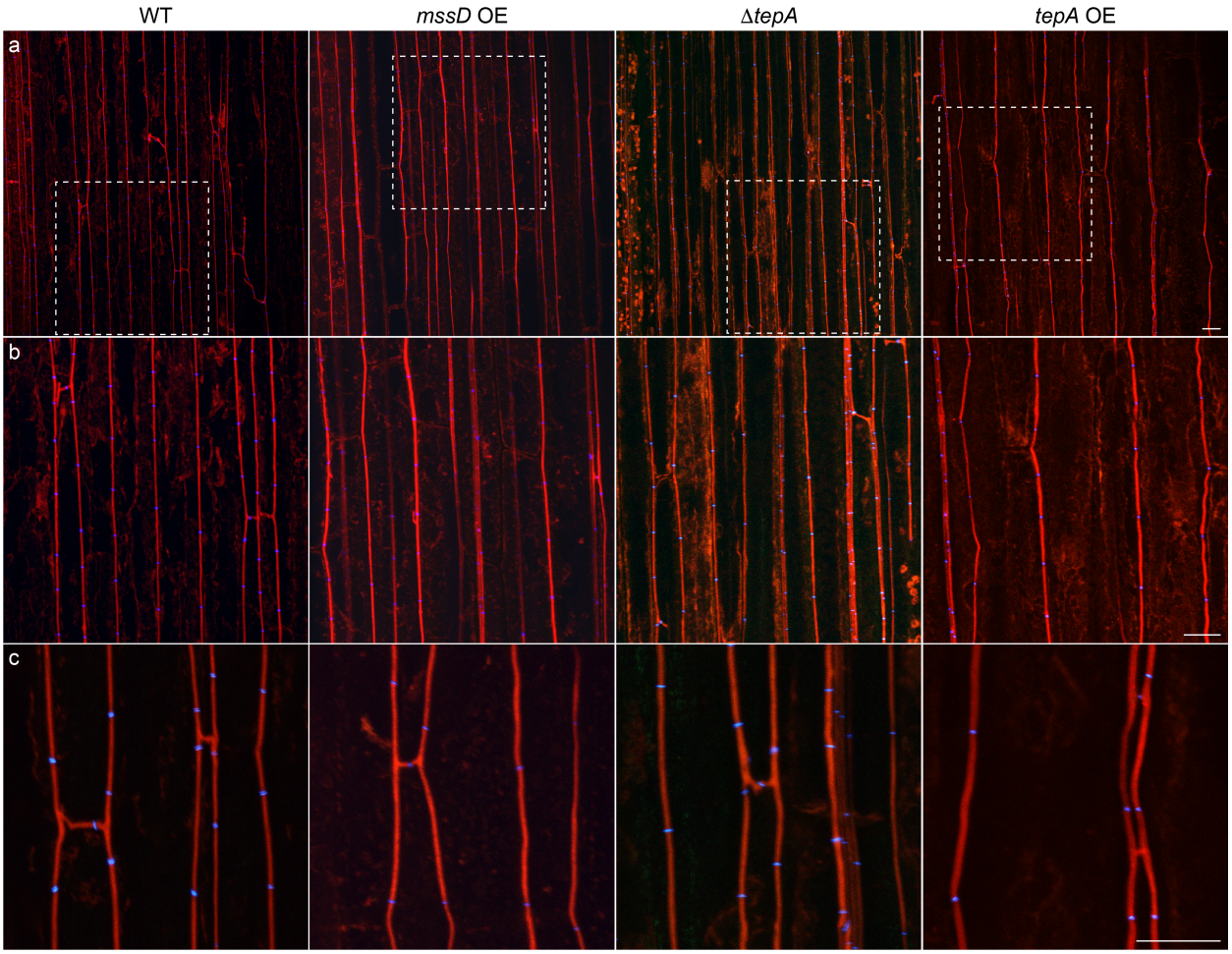

Fig. S10: Confocal depth series of longitudinal sections of *Lolium perenne* infected with *Epichloë festucae* wild-type and *mssD* and *tepA* mutant strains.

Infected *L. perenne* pseudostem samples were labelled with WGA-AF488 (chitin-binding, blue pseudocolour) and aniline blue (β-glucan-binding, red pseudocolour) and visualized with confocal scanning laser microscopy. Representative images of plant material infected with wild-type (WT), *mssD* overexpression (OE) #T17, Δ*tepA* #T87 and *tepA* OE #T7 strains. (a) Representative image (z = 6 µm) of strains *in planta;* Bar = 10 µm; (b) Magnified images of white boxed region in (a); Bar = 10 µm. (c) Higher magnification images (z = 4 µm) of hyphal branching and fusion. Bar = 10 µm.

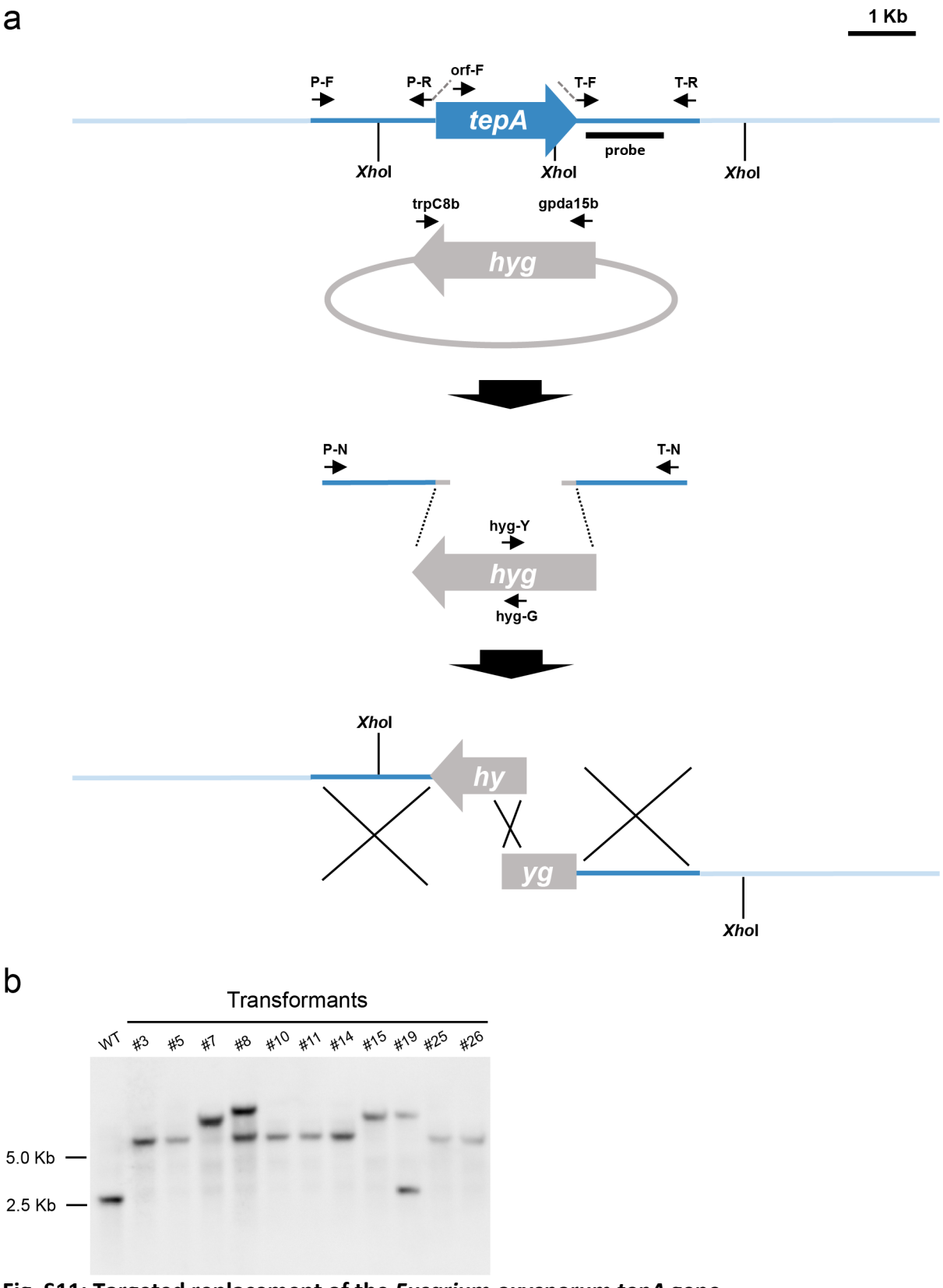

Fig. S11: Targeted replacement of the *Fusarium oxysporum tepA* gene.

(a) Physical maps of the *F. oxysporum tepA* locus and the split-marker gene replacement constructs obtained by fusion PCR. Relative positions of restriction sites and PCR primers are indicated. *hyg*, hygromycin resistance gene. (b) Southern blot analysis. Genomic DNA of the wild-type strain and eleven independent transformants was treated with *Xho*I, separated on a 0.7% agarose gel, transferred to a nylon membrane and hybridized with the DNA probe indicated in (a).

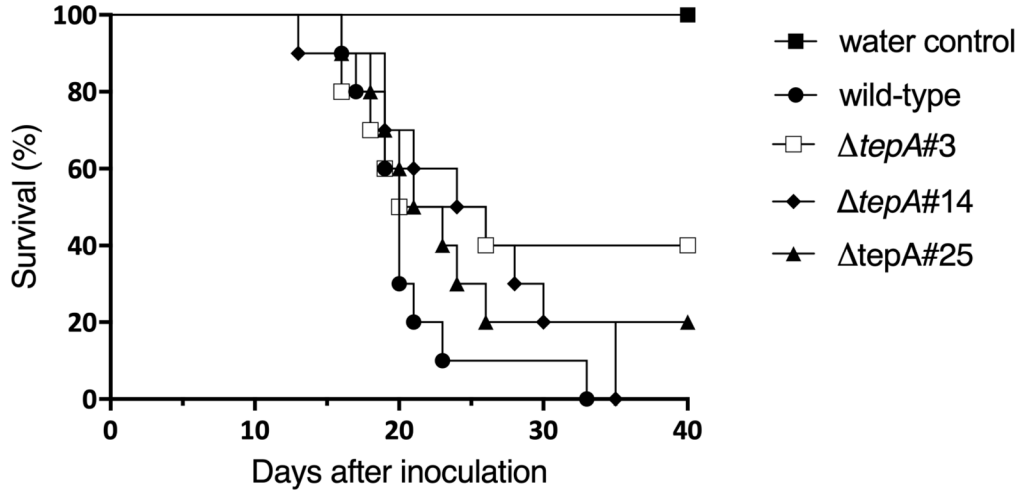

Fig. S12: TepA is not required for virulence of *Fusarium oxysporum*.
Roots of 2-week-old tomato plants were inoculated with 5 x 10^6 microconidia ml^{-1} of the indicated *F. oxysporum* strains and planted in minipots. Plant survival was recorded daily for 40 d. Data shown are from one representative experiment. All experiments were performed twice with similar results.

Table S1: Biological material.

Organism/Strain	Characteristics	Reference
E. coli		
DH5α	F⁻, ϕ80*lacZ*, ΔM15, Δ(*lacZYA-argF*), U169, *recA1*, *endA1*, *hsdR17* (r_k^-, m_k^-), *phoA*, *supE44*, λ⁻, *thi-1*, *gyrA96*, *relA1*	Invitrogen
E. festucae		
PN2278 (Fl1)	Wild-type isolated from *Festuca longifolia*	(Young et al., 2005)
E2368		(Schardl et al., 2013)
Δ*tepA* #T80	WT/Δ*tepA::*P*trpC-hph;* Hyg^R	This study
PN3278 (Δ*tepA* #T87)	WT/Δ*tepA::*P*trpC-hph;* Hyg^R	This study
PN3279 (Δ*tep*A #T102)	WT/Δ*epA::*P*trpC-hph;* Hyg^R	This study
Δ*tepA* #T87 PLC-GFP #TN1	Δ*tepA*#T87/pCE105/pII99, Hyg^R, Gen^R	This study
Δ*tepA* #T87 PLC-GFP #TN2	Δ*tepA*#T87/pCE105/pII99, Hyg^R, Gen^R	This study
Δ*tepA* #T87 BTK-GFP #15	Δ*tepA*#T87/pCE107/pII99, Hyg^R, Gen^R	This study
Δ*tepA* #T102 BTK-GFP #15	Δ*tepA*#T102/pCE107/pII99, Hyg^R, Gen^R	This study

tepA overexpression #T4	WT/pCE122, pSF16.17, Gen^R	This study
tepA overexpression #T7	WT/pCE122, pSF16.17, Gen^R	This study
tepA overexpression #T20	WT/pCE122, pSF16.17, Gen^R	This study
tepA overexpression #T7 PLC-GFP #T6	*tepA* overexpression#T7/pCE105/pBH12, Hyg^R, Gen^R	This study
tepA overexpression #T7 PLC-GFP #T11	*tepA* overexpression#T7/pCE105/pBH12, Hyg^R, Gen^R	This study
tepA overexpression #T7 BTK-GFP #T1	*tepA* overexpression#T7/pCE107/pBH12, Hyg^R, Gen^R	This study
tepA overexpression #T7 BTK-GFP #T2	*tepA* overexpression#T7/pCE107/pBH12, Hyg^R, Gen^R	This study
mssD overexpression #T17	WT/pCE101, pSF16.17, Gen^R	This study
mssD overexpression #T20	WT/pCE101, pSF16.17, Gen^R	This study
mssD overexpression #T53	WT/pCE101, pSF16.17, Gen^R	This study
mssD overexpression #T17 PLC-GFP #T20	WT/pCE101, pSF16.17, pCE105, pBH12, Gen^R, Hyg^R	This study
mssD overexpression #T17 BTK-GFP #T1	WT/pCE101, pSF16.17, pCE105, Gen^R, Hyg^R	This study
mssD overexpression #T17 BTK-GFP #T8	WT/pCE101, pSF16.17, pCE105, Gen^R, Hyg^R	This study
WT GFP-TepA #T4	WT/pBH41, Gen^R	This study
WT GFP-TepA #T5	WT/pBH41, Gen^R	This study
WT GFP-TepA #T9	WT/pBH41, Gen^R	This study
WT GFP-TepA #T15	WT/pBH41, Gen^R	This study
WT TepA-mCherry #T1	WT/pBH42, Hyg^R	This study
WT TepA-mCherry #T2	WT/pBH42, Hyg^R	This study
WT TepA-mCherry #T3	WT/pBH42, Hyg^R	This study
WT TepA-mCherry #T10	WT/pBH42, Hyg^R	This study
WT GFP-MssD #T2	WT/pBH72, Hyg^R	This study
WT GFP-MssD #T3	WT/pBH72, Hyg^R	This study
WT GFP-MssD #T8	WT/pBH72, Hyg^R	This study
WT GFP-MssD #T14	WT/pBH72, Hyg^R	This study
WT GFP-MssD #T16	WT/pBH72, Hyg^R	This study
WT GFP #T6	WT/pBH28, Gen^R	(Hassing et al., 2020)
WT GFP #T2	WT/pCE125, pSF16.17, Gen^R	This study
WT GFP #T8	WT/pCE125, pSF16.17, Gen^R	This study
WT mCherry #T1	WT/pCE126, pSF16.17, Gen^R	This study
WT mCherry #T2	WT/pCE126, pSF16.17, Gen^R	This study
WT PLC-GFP #T6	WT/pCE105/pSF16.17, Gen^R	This study
WT PLC-GFP #T12	WT/pCE105/pSF16.17, Gen^R	This study
WT PLC-GFP #T19	WT/pCE105/pSF16.17, Gen^R	This study
WT PLC-GFP #T2	WT/pCE105/pBH12, Hyg^R	This study
WT PLC-GFP #T3	WT/pCE105/pBH12, Hyg^R	This study
WT PLC-GFP #T7	WT/pCE105/pBH12, Hyg^R	This study
WT mCherry-PLC #T10	WT/pCE110/pSF16.17, Gen^R	This study
WT mCherry-PLC #T16	WT/pCE110/pSF16.17, Gen^R	This study
WT BTK-GFP #T9	WT/pCE107/pSF16.17, Gen^R	This study
WT BTK-GFP #T20	WT/pCE107/pSF16.17, Gen^R	This study
WT mCherry-BTK #T16	WT/pCE112/pSF16.17, Gen^R	This study
WT mCherry-BTK #T32	WT/pCE112/pSF16.17, Gen^R	This study
WT mCherry-BTK #T33	WT/pCE112/pSF16.17, Gen^R	This study
WT HGS-GFP #T9	WT/pCE106/pSF16.17, Gen^R	This study
WT HGS-GFP #T18	WT/pCE106/pSF16.17, Gen^R	This study
WT HGS-GFP #T24	WT/pCE106/pSF16.17, Gen^R	This study

WT mCherry-HGS #T5	WT/pCE111/pSF16.17, Gen^R	This study
WT mCherry-HGS #T22	WT/pCE111/pSF16.17, Gen^R	This study
WT mCherry-HGS #T37	WT/pCE111/pSF16.17, Gen^R	This study
WT PLEKHA2-GFP #T1	WT/pCE108/pSF16.17, Gen^R	This study
WT PLEKHA2-GFP #T4	WT/pCE108/pSF16.17, Gen^R	This study
WT mCherry-PLEKHA2 #T3	WT/pCE113/pSF16.17, Gen^R	This study
WT mCherry-PLEKHA2 #T37	WT/pCE113/pSF16.17, Gen^R	This study
WT mCherry-PLEKHA2 #T40	WT/pCE113/pSF16.17, Gen^R	This study
WT PLEKHA3-GFP #T3	WT/pCE109/pSF16.17, Gen^R	This study
WT PLEKHA3-GFP #T8	WT/pCE109/pSF16.17, Gen^R	This study
WT PLEKHA3-GFP #T37	WT/pCE109/pSF16.17, Gen^R	This study
WT mCherry-PLEKHA3 #T18	WT/pCE114/pSF16.17, Gen^R	This study
WT mCherry-PLEKHA3 #T25	WT/pCE114/pSF16.17, Gen^R	This study
WT mCherry-PLEKHA3, VPS52-GFP #T35	EFS30/pKG55, Gen^R, Hyg^R	This study
WT mCherry-PLEKHA3, VPS52-GFP #T43	EFS30/pKG55, Gen^R, Hyg^R	This study
WT mCherry-PLEKHA3 #T29	WT/pCE114/pSF16.17, Gen^R	This study
WT eGFP-ML1 #T5	WT/pBH87/pII99, Gen^R	This study
WT eGFP-ML1 #T6	WT/pBH87/pII99, Gen^R	This study
WT eGFP-ML1 #T15	WT/pBH87/pII99, Gen^R	This study
WT ML1-mCherry #T3	WT/pBH88/pII99, Gen^R	This study
WT ML1-mCherry #T6	WT/pBH88/pII99, Gen^R	This study
WT ML1-mCherry #T12	WT/pBH88/pII99, Gen^R	This study
E2368 PLC-GFP #T8	E2368/pCE105/pSF16.17, Gen^R	This study
E2368 PLC-GFP #T10	E2368/pCE105/pSF16.17, Gen^R	This study
E2368 mCherry-PLC #T5	E2368/pCE110/pSF16.17, Gen^R	This study
E2368 mCherry-PLC #T7	E2368/pCE110/pSF16.17, Gen^R	This study
E2368 BTK-GFP #T5	E2368/pCE107/pSF16.17, Gen^R	This study
E2368 mCherry-BTK #T1	E2368/pCE112/pSF16.17, Gen^R	This study
E2368 HGS-GFP #T7	E2368/pCE106/pSF16.17, Gen^R	This study
E2368 HGS-GFP #T36	E2368/pCE106/pSF16.17, Gen^R	This study
E2368 HGS-GFP #T44	E2368/pCE106/pSF16.17, Gen^R	This study
E2368 mCherry-HGS #T19	E2368/pCE111/pSF16.17, Gen^R	This study
E2368 mCherry-HGS #T29	E2368/pCE111/pSF16.17, Gen^R	This study
E2368 mCherry-HGS #T32	E2368/pCE111/pSF16.17, Gen^R	This study
E2368 PLEKHA2-GFP #T7	E2368/pCE108/pSF16.17, Gen^R	This study
E2368 PLEKHA2-GFP #T48	E2368/pCE108/pSF16.17, Gen^R	This study
E2368 PLEKHA2-GFP #T58	E2368/pCE108/pSF16.17, Gen^R	This study
E2368 mCherry-PLEKHA2 #T6	E2368/pCE113/pSF16.17, Gen^R	This study
E2368 mCherry-PLEKHA2 #T23	E2368/pCE113/pSF16.17, Gen^R	This study
E2368 mCherry-PLEKHA2 #T76	E2368/pCE113/pSF16.17, Gen^R	This study
E2368 PLEKHA3-GFP #T2	E2368/pCE109/pSF16.17, Gen^R	This study
E2368 mCherry-PLEKHA3 #T3	E2368/pCE114/pSF16.17, Gen^R	This study
E2368 mCherry-PLEKHA3 #T16	E2368/pCE114/pSF16.17, Gen^R	This study

E2368 mCherry-PLEKHA3 #T22	E2368/pCE114/pSF16.17, Gen^R	This study
E2368 GFP #T5	E2368/pCE125, pSF16.17, Gen^R	This study
E2368 GFP #T6	E2368/pCE125, pSF16.17, Gen^R	This study
E2368 GFP #T10	E2368/pCE125, pSF16.17, Gen^R	This study
E2368 GFP #T19	E2368/pCE125, pSF16.17, Gen^R	This study
E2368 mCherry #T7	E2368/pCE126, pSF16.17, Gen^R	This study
F. oxysporum		
4287	Wild-type *Fusarium oxysporum*, Race 2	
Δ*tepA* #3	Δ*tepA:hph;* Hyg^R	This study
Δ*tepA* #14	Δ*tepA:hph;* Hyg^R	This study
Δ*tepA* #25	Δ*tepA:hph;* Hyg^R	This study
Δ*tepA*/*tepA* #2	Δ*tepA:hph; tepA; pHleo;* Hyg^R Phleo^R	This study
Plasmid	**Characteristics**	**Reference**
PN1862 (pSF15.15)	pSP72 containing 1.4-kb *Hind*III P*trpC-hph* from pCB1004 cloned into *Sma*I site. Amp^R; Hyg^R; *Nco*I-free P*trpC-hph*	S. Foster
PN (pSF16.17)	P*trpC-nptII*-T*trpC*; AmpR; Gen^R	(Saikia and Scott, 2009)
PN4183 (pRS426)	*ori*(f1)-l*acZ*-T7 promoter-MCS (*Kpn*I-*Sac*I)-T3 promoter-*lacI*-*ori*(pMB1)-amp^R-*ori* (2 micron), *URA3;* Amp^R	(Christianson et al., 1992)
PN1687 (pII99)	P*trpC-nptII*-T*trpC*, Amp^R/Gen^R	(Lara-Ortiz et al., 2003)
PN4241 (pBV579)	pAN583 containing a 0.1 kb *Bsr*GI/*Bam*HI fragment containing NLS (three tandem repeats of the nuclear localisation signal from simian virus large T-antigen) from pEBFP2-Nuc	(Khang et al., 2010)
pPN82	pBlueScriptII® KS(+) containing 1.4-kb *Hind*III P*trpC-hph* and P*gpdA*-eGFP-T*trp*C; Amp^R /Hyg^R	(Tanaka et al., 2006)
pKG55	pPN94 containing P*tef-vps52-egfp*-T*trpC* (*vps52*: 2167 bp), Hyg^R	Green, pers. comm.
pCE101	pRS426 containing a P*gdpA-mssD*-T*trpC* overexpression construct	
pCE105	pRS426 containing a P*gpdA*-$PH_{PLC\text{-}\delta1}$-5Gly-eGFP-T*trpC* insert	This study
pCE107	pRS426 containing a P*gpdA*-PH_{BTK}-5Gly-eGFP-T*trpC* insert	This study
pCE105	pRS426 containing P*gpdA*- PLC PH domain-eGFP-T*trpC*; Amp^R	This study
pCE106	pRS426 containing P*gpdA*- HGS FYVE domain-eGFP-T*trpC*; Amp^R	This study
pCE107	pRS426 containing P*gpdA*- BTK PH domain-eGFP-T*trpC*; Amp^R	This study
pCE108	pRS426 containing P*gpdA*- PLEKHA2 PH domain-eGFP-T*trpC*; Amp^R	This study
pCE109	pRS426 containing P*gpdA*- PLEKHA3 PH domain-eGFP-T*trpC*; A Amp^R	This study
pCE110	pRS426 containing P*gpdA*-mCherry-PLC PH domain-T*trpC*; Amp^R	This study
pCE111	pRS426 containing P*gpdA*-mCherry-HGS FYVE domain-T*trpC*; Amp^R	This study
pCE112	pRS426 containing P*gpdA*-mCherry-BTK PH domain-T*trpC*; Amp^R	This study
pCE113	pRS426 containing P*gpdA*-mCherry PLEKHA2 PH domain-T*trpC*; Amp^R	This study
pCE114	pRS426 containing P*gpdA*-mCherry- PLEKHA3 PH domain-T*trpC*; Amp^R	This study
pCE122	pRS426 containing a P*gdpA-tepA*-T*trpC* overexpression construct	This study
pCE25	pRS426 containing a P*gpdA*-eGFP-T*trpC* insert	This study
pCE126	pRS426 containing a P*gpdA*-mCherry-T*trpC* insert	This study
pBH16	pBH12 containing mCherry-NLS amplified from pBV579	This study
pBH12	pPN94 containing 723 bp *B. cinerea tub* terminator insert amplified from pNR1 downstream of *hph*; Hyg^R	(Hassing et al., 2019)
pBH28	pBH12 containing *nptII* replacing *hph* and *egfp*; Gen^R	(Hassing et al., 2019)
pBH41	pBH28 containing P*gpdA-egfp-tepA*-T*trpC*, Gen^R	This study
pBH42	pBH12 containing P*gpdA-tepA-mCherry*-T*trpC*, Hyg^R	This study
pBH43	pRS426 containing the *tepA* deletion construct, Hyg^R	This study

pBH72	pBH12 containing P*tef-egfp-mssD*-T*trpC*, Hyg^R	This study
pBH87	pRS426 containing P*gpdA*- tandem repeat of ML1(1-86 bp) lipid binding domain-eGFP-T*trpC*; Amp^R	This study
pBH88	pRS426 containing P*gpdA*-mCherry- tandem repeat of ML1(1-86 bp) lipid binding domain-T*trpC*; Amp^R	This study

Table S2: Primers used in this study.

Name	Sequence (5'-3')	Purpose
tep5	ACAGCTACCCCGCTTGAGCAGACATCACCATGGCCTCGTTGTTGCGGCAG	*tepA* for overexpression construct
tep6	AGATTCGTCAAGCTGTTTGATGATTTCAGTTATTTCTGGCCATTCCCAAC	*tepA* for overexpression construct
BH60	GTTGACGGCAATTTCGATG	verification of deletion
BH75	CAGTGAGCGAGGAAGCGGAAGGCTTGCTTAGCTTGATATCTG	pBH12 amplification
BH76	CTGAAATCATCAAACAGCTTG	pBH12 amplification
BH79	GGAGGTGGAGGTTCTGGTGGAGGTGGATCTATGGTGAGCAAGGGCGAGGA	*mCherry* with linker forward
BH114	GTGACACTATAGAACTCGACGAATTCCCTTGTATCTCTACA	Amplification of P*gdpA+egfp* forward
BH191	CATAGATCCACCTCCACCAGAACCTCCACCTCCCTTGTACAGCTCGTCCATGC	Amplification of P*gdpA+egfp* with linker reverse
BH193	GTCGAGTTCTATAGTGTCACC	Amplification of vector backbone
BH195	GGAGGTGGAGGTTCTGGTGGAGGTGGATCTATGGCCTCGTTGTTGCGGCAG	Forward amplification of *tepA* with linker
BH196	GGTGATGTCTGCTCAAGCGG	Amplification of vector backbone
BH197	CTTCCGCTTCCTCGCTCACTG	Amplification of vector backbone
BH199	CAAGCTGTTTGATGATTTCAGTTAAGATCTGTACAGCTCGTCCATGCCG	*mCherry* reverse overhang to pBH12
BH203	CCGCTTGAGCAGACATCACCATGGCCTCGTTGTTGCGGCAG	*tepA* forward, overhang to P*gpdA*
BH204	CATAGATCCACCTCCACCAGAACCTCCACCTCCTTTCTGGCCATTCCCAACCAAG	*tepA* reverse, overhang to *mCherry*
BH208	GGGTTTTCCCAGTCACGACATCGATCTTCCGCGACGCAGAGTACAACT	*tepA* 3' flank for deletion
BH209	CCTTCAATATCAGTTCCAAGCTGTAGATTTTCTCATTGTTTC	*tepA* 3' flank for deletion
BH210	CGTCCGAGGGCAAAGGAATAGGCCTGCGTAGGAAAAGCGAGATTATG	*tepA* 5' flank for deletion
BH211	CAATTTCACACAGGAAACAGCATCGATGTCAACAAGTCAAGACACGCA	*tepA* 5' flank for deletion
BH212	TTACAGAGACCGAGGCGATC	verification of deletion
BH213	CGAGAGAAATCATTGCCCGG	verification of deletion
BH214	GAGAGAGAGAGAGAGAGAGAG	verification of deletion
BH215	CTTTGCTCTCCCCGTTGTC	verification of deletion
BH285	GTGCACCTATTTCCACAAG	verification of deletion
BH411	ATGGCCACCCCAGCAGGTAG	*ML1* for
BH412	GAGCATGAGCTTGCAGGGCTT	*ML1* rev
BH413	AAGCCCTGCAAGCTCATGCTCGGAGGAGGAGGAGGAATGGTGAGCAAG	*egfp* for with overhang to *ML1*
BH414	CTACCTGCTGGGGTGGCCATGGTGATGTCTGCTCAAGCGG	P*gpdA* rev with overhang to *ML1*
BH415	AAGCCCTGCAAGCTCATGCTCTAGCTGAAATCATCAAACAGCTTG	T*trpC* for with overhang to *ML1*
BH416	CACAGGAGGTACTAGACTACCTTTCATCCTACATAAATAGACG	pRS426 rev
BH417	GTAGTCTAGTACCTCCTGTGATATTATCCCATTCCATG	pRS426 for
BH418	CTACCTGCTGGGGTGGCCATTCCTCCTCCTCCTCCCTTGTACAGCTCGTCCATGC	*mCherry* rev with overhang to ML1
TtrpC-F	CTGAAATCATCAAACAGCTTGACG	T*trpC* for overexpression construct
pRS426-TtrpC-R	GCGGATAACAATTTCACACAGGAAACAGCCCATCTTAGTAGGAATGATTTTCG	T*trpC* for overexpression construct

pRS426-Pgdp-F	GTAACGCCAGGGTTTTCCCAGTCACGACGAATTCCCTTGTATCTCTACA	P*gpdA* for overexpression construct
Pgdp-R	GGTGATGTCTGCTCAAGCGGGGTAG	P*gpdA* for overexpression construct
pRS426_F	GCTGTTTCCTGTGTGAAATTG	pRS426 backbone
pRS426_R	GGGTTTTCCCAGTCACGAC	pRS426 backbone
hph_F	AGCTTGGAACTGATATTGAAGG	*hph* for deletion constructs
hph_R	CGTCCGAGGGCAAAGGAATAG	*hph* for deletion constructs
GlyGFP-F	GGAGGAGGAGGAGGAATGGTGAGCAAGGGCGAGGAG	*egfp* for molecular probe construct
mCherry-F	ACAGCTACCCCGCTTGAGCAGACATCACCATGGTGAGCAAGGGCGAGGAG	*mCherry* for molecular probe construct
hgs1	AGATTCGTCAAGCTGTTTGATGATTTCAGCTACTTCTTGTTGAGCTGCTC	*hgs* for mCherry molecular probe
hgs2	ACAGCTACCCCGCTTGAGCAGACATCACCATGGAGCGCGCCCCCGACTGGGTCG	*hgs* for eGFP molecular probe
hgs3	CCCTTGCTCACCATTCCTCCTCCTCCTCCCTTCTTGTTGAGCTGCTCGTAGC	*hgs* for eGFP molecular probe
plc1	AGATTCGTCAAGCTGTTTGATGATTTCAGCTACTGGCGCTGGTCCATGC	*plc* for mCherry molecular probe
plc2	ACAGCTACCCCGCTTGAGCAGACATCACCATGCTCCAGGACGACCCCGACCTCC	*plcs* for eGFP molecular probe
plc3	CCCTTGCTCACCATTCCTCCTCCTCCTCCCTGGCGCTGGTCCATGCTGC	*plc* for eGFP molecular probe
btk1	AGATTCGTCAAGCTGTTTGATGATTTCAGCTACTCGAGGATCTGGCAGCC	*btk* for mCherry molecular probe
btk2	ACAGCTACCCCGCTTGAGCAGACATCACCATGGCCGTCATCCTCGAGAGCATC	*btk* for eGFP molecular probe
btk3	CTTGCTCACCATTCCTCCTCCTCCCTCGAGGATCTGGCAGCCCATGG	*btk* for eGFP molecular probe
plekha2-1	AGATTCGTCAAGCTGTTTGATGATTTCAGCTAGGGGTGGCACTTGAGG	*plekha2* for mCherry molecular probe
plekha2-2	ACAGCTACCCCGCTTGAGCAGACATCACCATGACCGGCCCCCCCCTCATCAAG	*plekha2* for eGFP molecular probe
plekha2-3	GCCCTTGCTCACCATTCCTCCTCCTCCTCCGGGGTGGCACTTGAGGGCCTG	*plekha2* for eGFP molecular probe
plekha3-1	AGATTCGTCAAGCTGTTTGATGATTTCAGCTAGGTGAGGCAGGCCTTGC	*plekha3* for mCherry molecular probe
plekha3-2	ACAGCTACCCCGCTTGAGCAGACATCACCATGGAGGGCGTCCTCTACAAG	*plekha3* for eGFP molecular probe
plekha3-3	GCCCTTGCTCACCATTCCTCCTCCTCCTCCGGTGAGGCAGGCCTTGCTGC	*plekha3* for eGFP molecular probe
TepA-P-Fwd	ATAGTCGGTTGGTTTGTAGGG	*tepA* 5' flank for deletion
TepA-P-Nested	CCCCTCGCCTTGATCCCTT	*tepA* 5' nested for deletion
TepA-P-Rv	GAATGCACAGGTACACTTGTTTAGCGGTCGTCAAGTTGCGG	*tepA* reverse, overhang to *hph*
TepA-T-Fwd	AGGGGCTGTATTAGGTCTCGGATGTAAGACCATGAGTGTGAA	*tepA* forward, overhang to *hph*
TepA-T-Nested	AGTTGCTTGAGAATGTGAGGG	*tepA* 3' nested for deletion
TepA-T-Rv	CCTTGTGACCTTGCGTTTTATT	*tepA* 3' flank for deletion
TepA-orf-Fwd	GAGGCTGGCTTGGATTTGTG	PCR confirmation
gpdA15B	CGAGACCTAATACAGCCCCT	*hph* for deletion constructs
trpterC8B	AAACAAGTGTACCTGTGCATTC	*hph* for deletion constructs
gpdA16B	AGGGGCTGTATTAGGTCTCG	confirmation knockout
trpC4B	CCTGGGTTCGCAAAGATAATT	confirmation knockout
Hyg-G	CGTTGCAAGACCTGCCTGAA	*hph* for deletion constructs
Hyg-Y	GGATGCCTCCGCTCGAAGTA	*hph* for deletion constructs
Primers used for RT-qPCR.		
BH189	GAGGAGATTCTGGAACCGGC	*tepA* forward
BH190	CCTCGGCATCATCGTCATCA	*tepA* reverse
AC33	TGCGTGACAAAACTCTCCAG	*mssD* forward

AC34	AGCCTTTCTCACGTTCTCCA	*mssD* reverse
TC399	AAAAAGCAACCGAATGCAAG	*EF-2* forward
TC400	CGAGACGACATAACTACATGTATCAAA	*EF-2* reverse
TC407	TAGCTGGCGTTATGGAAAGG	*S22* forward
TC408	CGATTGTGCGACTACTACCTCA	*S22* reverse
YL113F	GAGAATTCCAGCCACGCTAC	*pacC* forward
YL113R	AACCATCACCAGGCAAAGAC	*pacC* reverse
YL120F	ATGCAACAAAACGTTCACGA	*hepA* forward
YL120R	GCTGCTTTCCTCCTCACAAG	*hepA* reverse
YL501R	TGAAGAGCCTCCAGGAGAAG	*LpCCR1* forward
YL501F	CCTCATGCTCGGATGGTAAC	*LpCCR1* reverse
YL502F	CTGGTACTGCTACGGGAAGG	*LpCCR1* forward
YL502R	TCACCACCACAAGGTCCAC	*LpCCR1* reverse

Methods S1: Construct design.

For the generation of the lipid molecular probes, the mouse lipid-binding domains (LBDs) were codon-optimised for expression in fungi using codon usage information generated for *E. festucae* (Schardl et al., 2013). Codon-optimised LBDs were fused to mCherry at the N-terminus with a 6x glycine linker generated as inserts in the vector pUC57 by GenScript USA Inc. (Piscataway, USA). The LBD was then amplified from these constructs and fused to eGFP at the C-terminus with a 5x glycine linker using Gibson assembly. Gibson assembly was further used to clone the mCherry-6Gly-LBD and LBD-5Gly-eGFP fragments under the control of the *Aspergillus nidulans gpdA* promoter and *trpC* terminator, to generate either P*gpdA*-mCherry-6Gly-LBD-T*trpC* or P*gpdA*-LBD-5Gly-eGFP-T*trpC* fragments within pRS426. The ML1 lipid-binding domain was ordered as codon-optimised tandem repeat sequence from Twist Bioscience (San Francisco, USA) and amplified with BH411/BH412. For the eGFP fusion construct the backbone was amplified in two fragments from other LPD-eGFP fusion constructs with BH413/416 and BH417/414. For the mCherry fusion construct, the backbone was amplified in two fragments from other LPD-mCherry fusion constructs with BH411/418 and BH415/416. The fragments were assembled by Gibson assembly.

For the generation of the *mssD* deletion construct (pCE98), a 1208-bp PCR fragment 5' of *mssD* and a 1020-bp PCR fragment 3' of *mssD* were amplified with the mssD1/mssD2 and mssD3/mssD4 primer pairs, respectively, from Fl1 genomic DNA. For the generation of the *tepA* replacement construct (pBH43), a 1,269-bp PCR fragment 5' of *tepA* and a 1291-bp PCR fragment 3' of *tepA* were amplified from Fl1 genomic DNA with the primer pairs BH210/BH211 and BH208/BH209, respectively. The pRS426 backbone was amplified with the pRS426 backbone F/pRS426 backbone R (5505 bp) primer pair, and the hygromycin resistance cassette P*trpC-hph* (1394 bp) from pSF15.15 with the primer combination hph_F/hph_R. For the replacement of *mssD*, a split marker approach (Rahanama et al., 2017) was employed in which the *mssD* replacement fragment was amplified as two pieces (mss1/hph-split-R 2025 bp; hph-split-F/mss4 2155 bp) with a 501-bp overlap in the middle of the *hph* resistance cassette. To generate the *mssD* overexpression (OE) construct (pCE101), the 3,029-bp *mssD* coding sequence was amplified with the primer pair mss5/mss6, while for the *tepA* overexpression construct, pCE122, *tepA* (1,798 bp) was amplified from Fl1 genomic DNA with the primer combination tep5/tep6. P*gpdA* and T*trpC* were amplified with the primer pairs pRS426-Pgdp-

F/pRS426-Pgdp-R (2310 bp) and TtrpC-F/pRS426-TtrpC-R (569 bp) from pPN82 and pII99, respectively. The pRS426 backbone was amplified with the primer combination pRS426 backbone F/pRS426 backbone R (5505 bp). Subsequently, all fragments were assembled using Gibson assembly.

The C-terminal mCherry fusion protein encoding constructs were assembled from three backbone fragments and the *tepA* (pBH42) coding region. The *tepA* coding region was amplified from Fl1 genomic DNA with the primer pair BH203/BH204. The backbone fragments included: a 2,817-bp fragment amplified from pBH16 with the primer pair BH76/BH75, containing T*trpC* and a *hph* cassette, a 4,608-bp fragment amplified from pBH28 with the primer pair BH197/196 containing genes for replication in *E. coli* and P*gpd*, and a 765-bp fragment amplified from pBV579 with the primer pair BH79/BH199 encoding *mCherry*. For the *tepA* N-terminal eGFP fusion protein constructs, the backbone was amplified in two fragments from pBH28. One fragment was 4,810 bp in length and was amplified with the primer pair BH76/BH193, and the other one was 3,080 bp in length and was amplified with the primer pair pBH114/BH191. For the *mssD* N-terminal GFP fusion construct, the backbone was assembled from the same 4,810 bp fragment in addition to a 717-bp fragment (*egfp*) amplified from pBH28 with the primer pair BH263/BH191 and a 795-bp fragment (P*tef*) amplified from pBH12 with the primer pair BH254/BH77. The 1,798-bp *tepA* coding region was amplified with BH195/tep6 and the 3,028-bp *mssD* coding region with the primer pair BH259/BH260. All fusion protein constructs encode a $(GGGS)_2$ linker between the protein of interest and the fluorophore.

In *Fusarium oxysporum*, targeted gene replacement with the hygromycin resistance cassette and complementation of the mutants by co-transformation with the phleomycin resistance cassette were performed as previously reported (Lopez-Berges et al., 2010). Briefly, two fragments encompassing approximately 2 kb of 5'- and 3'-flanking regions, respectively, were amplified using PCR with primer pairs TepA-P-Fwd/TepA-P-Rv and TepA-T-Fwd/TepA-T-Rv (Supplemental Figure 10 and Supplemental Table 2). The amplified fragments were then fused to overlapping parts of the hygromycin resistance cassette previously amplified with primers gpda15B/trpC8B, using the following primer combinations: TepA-P-Nested/HygG and HygY/TepA-T-Nested. PCR reactions were routinely performed with the High Fidelity Template PCR system (Roche Diagnostics, Barcelona, Spain), using a MJ Mini personal thermal cycler (Bio-Rad, Alcobendas, Spain). The two PCR products generated were used to transform protoplasts of *F. oxysporum* wild-type strain as described. Hygromycin resistant (Hyg^R) transformants were subjected to two rounds of monoconidial isolation. Deletion mutants were initially identified by PCR with primer pairs TepA-P-Fwd/TrpC4B and GpdA16B/TepA-T-Rv and the homologous recombination event was confirmed by Southern analysis. For complementation of the *F. oxysporum* Δ*tepA* mutant, a 5.0-kb fragment containing the *tepA* gene including promoter and terminator regions, was amplified from wild-type genomic DNA using primer pair TepA-P-Nested/TepA-T-Nested. A 2.5-kb fragment containing the phleomycin resistance (Phl^R) cassette was amplified using the primers gpda15B and trpC8B. Both fragments were used in the proportion 3:1 to co-transform protoplasts of the Δ*tepA* #3 mutant strain. Phleomycin resistant transformants were subjected to two rounds of monoconidial isolation and the presence of the wild type *tepA* gene was confirmed by PCR with primer pair TepA-orf-fwd/TepA-T-Rv.

References

Christianson, T.W., Sikorski, R.S., Dante, M., Shero, J.H., and Hieter, P. (1992). Multifunctional yeast high-copy-number shuttle vectors. Gene 110, 119-122.

Hassing, B., Eaton, C.J., Winter, D., Green, K.A., Brandt, U., Savoian, M.S., Mesarich, C.H., Fleissner, A., and Scott, B. (2020). Phosphatidic acid produced by phospholipase D is required for hyphal cell-cell fusion and fungal-plant symbiosis. Mol Microbiol 113, 1101-1121.

Hassing, B., Winter, D., Becker, Y., Mesarich, C.H., Eaton, C.J., and Scott, B. (2019). Analysis of Epichloe festucae small secreted proteins in the interaction with Lolium perenne. PLoS One 14, e0209463.

Khang, C.H., Berruyer, R., Giraldo, M.C., Kankanala, P., Park, S.Y., Czymmek, K., Kang, S., and Valent, B. (2010). Translocation of Magnaporthe oryzae effectors into rice cells and their subsequent cell-to-cell movement. Plant Cell 22, 1388-1403.

Lara-Ortiz, T., Riveros-Rosas, H., and Aguirre, J. (2003). Reactive oxygen species generated by microbial NADPH oxidase NoxA regulate sexual development in Aspergillus nidulans. Mol Microbiol 50, 1241-1255.

Lopez-Berges, M.S., Rispail, N., Prados-Rosales, R.C., and Di Pietro, A. (2010). A nitrogen response pathway regulates virulence functions in Fusarium oxysporum via the protein kinase TOR and the bZIP protein MeaB. Plant Cell 22, 2459-2475.

Lukito, Y., Chujo, T., and Scott, B. (2015). Molecular and cellular analysis of the pH response transcription factor PacC in the fungal symbiont Epichloë festucae. Fungal Genetics and Biology 85, 25-37.

Saikia, S., and Scott, B. (2009). Functional analysis and subcellular localization of two geranylgeranyl diphosphate synthases from Penicillium paxilli. Mol Genet Genomics 282, 257-271.

Schardl, C.L., Young, C.A., Hesse, U., Amyotte, S.G., Andreeva, K., Calie, P.J., Fleetwood, D.J., Haws, D.C., Moore, N., Oeser, B., et al. (2013). Plant-symbiotic fungi as chemical engineers: multi-genome analysis of the Clavicipitaceae reveals dynamics of alkaloid loci. PLoS Genet 9, e1003323.

Tanaka, A., Christensen, M.J., Takemoto, D., Park, P., and Scott, B. (2006). Reactive oxygen species play a role in regulating a fungus-perennial ryegrass mutualistic interaction. Plant Cell 18, 1052-1066.

Young, C.A., Bryant, M.K., Christensen, M.J., Tapper, B.A., Bryan, G.T., and Scott, B. (2005). Molecular cloning and genetic analysis of a symbiosis-expressed gene cluster for lolitrem biosynthesis from a mutualistic endophyte of perennial ryegrass. Mol Genet Genomics 274, 13-29.